Dark Matter Phenomenology in 2HDMS

Gudrid Moortgat-Pick*[1,2], Juhi Dutta[1], Cheng Li[2], Merle Schreiber[1,2], Tabira Sheikh[1], Julia Ziegler[1]

[1] *II. Inst. of Theo. Phys., University of Hamburg, Luruper Chaussee 149, 22761 Hamburg, Germany*
[2] *Deutsches Elektronen Synchrotron, DESY, Notkestr. 85, 22607 Hamburg,Germany*

The constituents of dark matter are still an unresolved puzzle. Several Beyond Standard Model (BSM) Physics offer suitable candidates. In this study here we consider the Two Higgs Doublet model augmented with a complex scalar singlet (2HDMS) and focus on the dark matter phenomenology of 2HDMS with the complex scalar singlet as the dark matter candidate. The parameter space allowed from existing experimental constraints from dark matter, flavour physics and collider searches has been studied. The discovery potential for such a 2HDMS at HL-LHC and at future e^+e^- colliders has been worked out.

1. Introduction

Dark Matter (DM) remains an unsolved puzzle at the interface between particle physics and cosmology, only 4-5% of the Universe are composed by 'known' matter components, but about 25% is built of dark matter. Since the Standard Model (SM) does not accommodate a suitable DM candidate, several Beyond Standard Model (BSM) extensions have been proposed to accommodate DM candidates ranging from scalar, fermion to vector candidates and with mass scales from below eV up to TeV particles. We concentrate in this contribution on thermal weakly interacting massive particles (WIMP) that is expected in the mass range of GeV up to TeV, accessible at future collider experiments at the LHC and a high-energy e^+e^- linear collider (ILC, CLIC).

Among popular BSM candidates are models extended via singlet scalars which provide a natural candidate for DM. While such extensions of SM [1] are strongly constrained via direct detection searches as well as the invisible branching ration of the 125 GeV SM-like Higgs, extended Higgs sector models such as the Two Higgs Doublet model (2HDM) [2] provides a dark matter candidate within the Inert Doublet model [2]. An alternate candidate for dark matter in such multi-Higgs models are minimal extensions with singlet scalars with the singlet scalar as the DM candidate. Such models have also the potential to explain the matter-antimatter asymmetry and to accomodate both inflation as well as gravitational waves phenomenology [3, 4] Such extensions involving real scalar singlets have been extensively studied [5–7] while complex scalar extensions to the 2HDM have also been recently studied in the context of modified Higgs sectors [8].

2. Extended Two Higgs Doublet Model

2.1 Symmetries

We consider the CP-conserving softly broken Type II Two Higgs Doublet model augmented with a complex scalar singlet (2HDMS) [8] consistent with flavour changing neutral currents (FCNCs) at tree-level. It allows for the presence of the mixing term between the two Higgs doublets, Φ_1 and Φ_2, i.e., m_{12}^2 while the explicit Z_2 breaking terms are absent. The complex scalar singlet S is stabilised by a Z_2' symmetry such that S is odd under Z_2' while the SM fields are even under the new Z_2' symmetry. The fields Φ_1 and S are even under Z_2 while Φ_2 is odd under Z_2.

We consider the case where Z_2' remains unbroken both explicitly and dynamically, i.e. the scalar

singlet doesn't obtain a vacuum expectation value. Therefore, the scalar potential V with a softly broken Z_2- and a conserved Z_2' symmetry is $V = V_{2HDM} + V_S$, where, the softly broken Z_2-symmetric 2HDM potential is:

$$V_{2HDM} = m_{11}^2\Phi_1^\dagger\Phi_1 + m_{22}^2\Phi_2^\dagger\Phi_2 + (m_{12}^2\Phi_1^\dagger\Phi_2 + h.c) + \tfrac{\lambda_1}{2}(\Phi_1^\dagger\Phi_1)^2 + \tfrac{\lambda_2}{2}(\Phi_2^\dagger\Phi_2)^2 \quad (1)$$

$$+\lambda_3(\Phi_1^\dagger\Phi_1)(\Phi_2^\dagger\Phi_2) + \lambda_4(\Phi_1^\dagger\Phi_2)(\Phi_2^\dagger\Phi_1) + [\tfrac{\lambda_5}{2}(\Phi_1^\dagger\Phi_2)^2 + h.c] \quad (2)$$

and the Z_2'-symmetric singlet potential, V_S, is

$$V_S = m_S^2 S^* S + (\tfrac{m_S^{2'}}{2}S^2 + h.c) + (\tfrac{\lambda_1''}{24}S^4 + h.c) + (\tfrac{\lambda_2''}{6}(S^2S^*S) + h.c) + \tfrac{\lambda_3''}{4}(S^*S)^2 \quad (3)$$

$$+S^*S\,[\lambda_1'\Phi_1^\dagger\Phi_1 + \lambda_2'\Phi_2^\dagger\Phi_2] + [S^2(\lambda_4'\Phi_1^\dagger\Phi_1 + \lambda_5'\Phi_2^\dagger\Phi_2) + h.c.]. \quad (4)$$

The doublet fields have the components $\Phi_1 = (h_1^+, \frac{1}{\sqrt{2}}(v_1 + h_1 + ia_1))^T$, $\Phi_2 = (h_2^+, \frac{1}{\sqrt{2}}(v_2 + h_2 + ia_2))^T$, $S = \frac{1}{\sqrt{2}}(h_s + ia_s)$ with $\tan\beta = \frac{v_2}{v_1}$ is the ratio of the up-type and down-type Higgs doublet vevs $v_{1,2}$ (with $v(= v_1^2 + v_2^2) \simeq 246$ GeV. Under the assumption that the complex singlet scalar does not develop a *vev* —for this study imposed—, the Higgs sector, after EWSB, remains the same as in 2HDM, i.e, consisting of two CP-even neutral scalars Higgses h, H, a pseudoscalar Higgs A and a pair of charged Higgses $H^\pm$ [2]. The Higgs-dark-matter portal couplings are given by $\lambda_{hSS*} \sim i/\sqrt{1+\tan^2\beta}(\lambda_1' \sin\alpha - \lambda_2' \cos\alpha \tan\beta)$ and $\lambda_{HSS*} \sim -i/\sqrt{1+\tan^2\beta}(\lambda_1' \cos\alpha + \lambda_2' \sin\alpha \tan\beta)$.

2.2 Theoretical and Phenomenological Constraints

The Sylvester's criterion and copositivity [9,10] has been applied to guarantee boundedness from below for the Higgs potential, leading to constraints on all coupling parameters λ, λ', λ''. The mass of the lightest CP-even Higgs particle $m_h = 125$ GeV has been chosen to be in concordance with the measured Higgs state via HiggsSignals and collider constraints from LEP and LHC have been applied for the heavy Higgs states via HiggsBounds. The branching ratio $BR(h \to \chi\chi) < 0,11$ (< 0.19), fulfilling the limits from ATLAS (CMS). Electroweak precision constraints on STU parameters have been taken into account as well as constraints from flavour physics $BR(b \to s\gamma)$, $BR(B_s \to \mu^+\mu^-)$, using SPheno. $\Delta(g_\mu - 2)$. Concerning the dark matter particle, the bounds on the relic density from PLANCK measurements $\Omega h^2 = 0.119$ as well as constraints from direct detection (XENON-1T) and indirect detection (FERMI-LAT) experiments have been applied using micrOMEGAs.

3. Results

3.1 Benchmark Points

This model has been implemented using SARAH code implemented into SPheno for the spectrum generation. In order to calculate collider observables the code chain Madgraph-Pythia-Delphes-Madanalysis has been used.

As can be seen from Figs.1a) and b) the mass of the dark matter particle χ as well as the coupling λ_2' get strongest constraints from the direct detection search from XENON-1T: in the shown example where the heavier Higgs particles are about 725 GeV, the mass $m_\chi \sim 338$ GeV. Scanning the available parameter space allowed to specifiy different benchmark areas, see Table3.2.2. BP1 and BP3 are very similar, however, they differ significantly in the couplings λ_1', λ_2' and λ_3 leading to different collider phenomenology.

3.2 Collider Phenomenology

In this section, we discuss the potential signals of this model at HL-LHC and future e^+e^- colliders. As already mentioned, the presence of the invisible decay of the heavy Higgs to the dark matter

candidate is a source of missing energy at colliders. Therefore, direct production of heavy Higgses and consequent decay of the Higgs to χ along with visible SM particles can give rise to distinct signatures for this scenario as opposed to the 2HDM like scenario. We investigate these possibilities and their prospects in the context of $\sqrt{s} = 14$ TeV LHC at the targeted integrated luminosity of 3-4 ab^{-1} and in future e^+e^- colliders (ILC,CLIC) up to $\sqrt{s} = 3$ TeV and integrated luminosities 5 ab^{-1}.

3.2.1 Prospects at LHC

The main processes contributing to neutral Higgs production at the LHC are gluon fusion (mediated by the top quark loop), vector boson fusion (VBF), associated Higgs production (Vh_i), $b\bar{b}h_i$, $t\bar{t}h_i$ [2]. For the charged Higgs pair, the possible production channels are H^+H^- and $W^\pm H^\mp$ [2]. At LHC Run 3 at $\sqrt{s} = 14$ TeV, all possible Higgs production processes (including SM and BSM Higgses) are summarised in Table 3.2.2.

In presence of the heavy Higgs H decaying to two dark matter candidates, one could obtain invisible momentum in the final state. Keeping this in mind, one can look into the following final states:

a) $1j$ (ISR)+missing E_T [12]

b) $2j + missing E_T$ [13]

We estimate the significance for the mono-jet and VBF channels using the cuts from an existing cut-and-count analyses performed in Ref [7] for $\sqrt{s} = 14$ TeV LHC, further details see [11]. For a) we obtain a cut efficiency for the signal in BP3 of about $\sim 18\%$ and we obtain a 0.111σ excess at 3ab^{-1} using gluon fusion production channel (at leading order (LO)). For b) we get a signal efficiency of 4.5% for BP3 and a signal significance of about $\sim 0.2\,\sigma$ at 3 ab^{-1}. Therefore, we observe that owing to the small invisible branching ratio and heavy Higgs masses ~ 820 GeV (and hence small production cross section) in BP3, the final states will be inaccessible at the upcoming HL-LHC run.

3.2.2 Prospects at a high-energy e^-e^+ Linar Collider (ILC, CLIC)

The cleaner environment and lesser background along the beam line compared to hadron colliders make the electron positron linear colliders an attractive choice for precision studies of new physics.

The International Linear Collider (ILC) [17] , is a proposed e^+e^- collider with simultanouesly polarized $e^\pm$ beams and a center-of-mass energies at the SM-like Higgs threshold ($\sqrt{s} = 250$ GeV), top threshold ($\sqrt{s} = 350$ GeV) and further upgrades such that the center of mass energies are $\sqrt{s} = 500$ GeV and up to $\sqrt{s} = 1$ TeV with a maximum target integrated luminosity of $\mathcal{L} = 500$ fb^{-1}. The othe proposed high-energy e^+e^- linear collider design is CLIC [14, 15] with an energy upgrade up to $\sqrt{s} = 1.5, 3$ TeV and at least a polarized e^-beam. An overview of the physics potential at future high-energy linear colliders is given in [20]. ILC (CLIC) gain advantage over the LHC in the possibility of exploiting the polarisation of the beams crucial both at the high energy stages but also already at the first stage of $\sqrt{s} = 250$ GeV [16, 19]. Although the invisible decay in BP3 is $H \to \chi\bar{\chi} \simeq 4.8\%$ and the low production cross section times branching ratio, we observe that the $2b + missing E_T$ channel is observable with a = 3.99σ significance at integrated luminosity $\mathcal{L} = 5$ ab^{-1}.

4. Conclusions and Outlook

We have studied dark matter phenomenology in a Two Higgs Doublet model with a complex scalar singlet where the scalar singlet doesn't obtain a vacuum expectation value. Benchmark scenarios consistent with all current experimental and cosmological constraints have been worked out. Particular stringent bounds on the available parameter range for the couplings are set by bounds from the direct detection. Due to very small rates of the heavy Higgs production, the dark matter candidates will probably not be detectable via monojet or di-jet studies even at the HL-LHC. However, at a high-energy linear collider with polarized beams and precise initial energy such a dark matter scenario

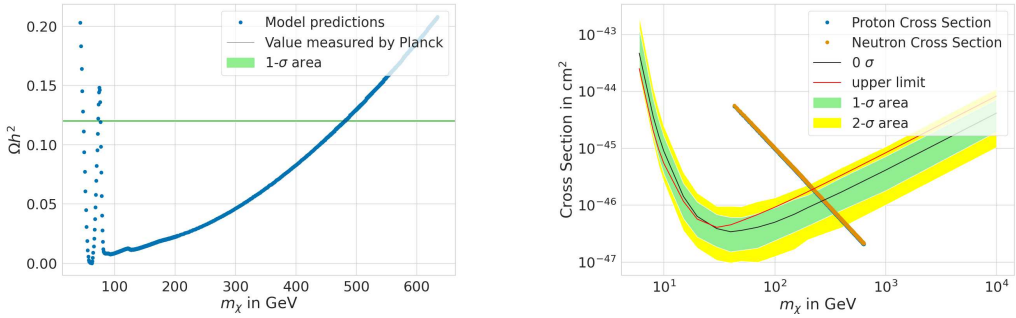

Fig. 1.: Relic density and direct detection cross-section predicted by the model depending on the DM mass m_χ [11]. The parameter m_S^2 has been varied.

Parameters	**BP1**	**BP2**	**BP3**
λ_1	0.23	0.1	0.23
λ_2	0.25	0.26	0.26
λ_3	0.39	0.10	0.2
λ_4	-0.17	-0.10	-0.14
λ_5	0.001	0.10	0.10
m_{12}^2(GeV^2)	-1.0×10^5	-1.0×10^5	-1.0×10^5
λ_1''	0.1	0.1	0.1
λ_3''	0.1	0.1	0.1
λ_1'	0.042	0.04	2.0
λ_2'	0.042	0.001	0.01
λ_4'	0.1	0.1	0.1
λ_5'	0.1	0.1	0.1
tanβ	4.9	6.5	6.5
m_h (GeV)	125.09	125.09	125.09
m_H(GeV)	724.4	816.4	821.7
m_A(GeV)	724.4	812.6	817.9
$m_{H^\pm}$ (GeV)	816.3	816.3	822.2
m_χ(GeV)	338.0	76.7	323.6
Ωh^2	0.058	0.119	0.05
$\sigma_p^{SI} \times 10^{10}$ (pb)	0.76	0.052	2.9
$\sigma_n^{SI} \times 10^{10}$ (pb)	0.78	0.054	3.1

Table I.: Relevant parameters of the benchmark points used for the study [11].

Processes	Cross section (in fb) at $\sqrt{s}$ = 14 TeV		
	BP1	**BP2**	**BP3**
h (ggF)	29.3×10^3	29.3×10^3	29.3×10^3
H	22.61	5.238	6.632
A	35	8.58	10.8
hjj (VBF)	1.296×10^3	1.265×10^3	1.25×10^3
Hjj	1.843	1.845	0.56
Ajj	2.885	2.88	40.91
Wh	1.148×10^3	1.133	1.134 pb
WH	1.195×10^{-3}	1.11e-03	1.199×10^{-3}
WA	4.3×10^{-4}	5.892e-04	5.734×10^{-4}
Zh	880.8	677.2	697.9
ZH	0.93	0.2783	0.3408
ZA	3.999	1.413	1.689
bbh	2534	2541	2541 pb
bbH	21.52	17.92	17.92 fb
bbA	23.39	18.9	19.04fb
$t\bar{t}h$	478.3	477.1	477.9
$t\bar{t}H$	0.1988	0.06571	0.7891
$t\bar{t}A$	0.2552	0.08036	0.09826
H^+H^-	0.06603	0.03033	0.03416
$W^\pm H^\mp$	102.4	3.453	4.145
$\chi\bar{\chi} + 1j$	0.006356	0.0681	0.8819

Table II.: The leading order (LO) cross section (in fb), further details see [11].

might be detectable. In addition, the option of direct dark matter pair production plus an ISR-photon is still under studies and offer another interesting possibility. Further studies on exploring the mixing angles in the Higgs sector to shed light on the dark matter behaviour is still ongoing.

Acknowledgments

JD and GMP acknowledge support by the Deutsche Forschungsgemeinschaft (DFG, German Research Foundation) under Germany's Excellence Strategy EXC 2121 "Quantum Universe"- 390833306.

References

[1] V. Barger, P. Langacker, M. McCaskey, M. Ramsey-Musolf and G. Shaughnessy, Phys. Rev. D **79** (2009), 015018 [arXiv:0811.0393 [hep-ph]].

[2] G. C. Branco, P. M. Ferreira, L. Lavoura, M. N. Rebelo, M. Sher and J. P. Silva, Phys. Rept. **516** (2012), 1-102 [arXiv:1106.0034 [hep-ph]].

[3] Dorsch, G. C. and Huber, S. J. and Konstandin, T. and No, J. M., JCAP **05** (2017), 052 [arXiv:1611.05874 [hep-ph]].

[4] Biekötter, Thomas and Olea-Romacho, María Olalla, JHEP **10** (2021), 215 [arXiv: 2108.10864 [hep-ph]].

[5] B. Grzadkowski and P. Osland, Phys. Rev. D **82** (2010), 125026 [arXiv:0910.4068 [hep-ph]].

[6] A. Drozd, B. Grzadkowski, J. F. Gunion and Y. Jiang, JHEP **11** (2014), 105 [arXiv:1408.2106 [hep-ph]].

[7] A. Dey, J. Lahiri and B. Mukhopadhyaya, JHEP **09** (2019), 004 [arXiv:1905.02242 [hep-ph]].

[8] S. Baum and N. R. Shah, JHEP **12** (2018), 044, [arXiv:1808.02667 [hep-ph]].

[9] Klimenko, K. G., Theor. Math. Phys. **62** (1985), 58.

[10] Kannike, Kristjan, Eur. Phys. J. C. **72** (2012), 2093, [arXiv: 1205.3781 [hep-ph]].

[11] J. Dutta, G. Moortgat-Pick and M. Schreiber, [arXiv:2203.05509 [hep-ph]].

[12] G. Aad *et al.* [ATLAS], Phys. Rev. D **103** (2021) no.11, 112006, [arXiv:2102.10874 [hep-ex]].

[13] [ATLAS], "Search for invisible Higgs boson decays with vector boson fusion signatures with the ATLAS detector using an integrated luminosity of 139 fb^{-1}," ATLAS-CONF-2020-008.

[14] P. N. Burrows *et al.* [CLICdp and CLIC], [arXiv:1812.06018 [physics.acc-ph]].

[15] A. Robson and P. Roloff, [arXiv:1812.01644 [hep-ex]].

[16] G. Moortgat-Pick, *et al.* Phys. Rept. **460** (2008), 131-243, hep-ph/0507011.

[17] C. Adolphsen, *et al.* arXiv:1306.6328; C. Adolphsen, *et al.* arXiv:1306.6353.

[18] P. Bechtle, S. Heinemeyer, O. Stal, T. Stefaniak and G. Weiglein, JHEP **1411** (2014) 039.

[19] K. Fujii, *et al.* arXiv:1801.02840.

[20] G. Moortgat-Pick, *et al.* Eur. Phys. J. C **75** (2015) no.8, 371, arXiv:1504.01726;